Benha Journal of Applied Sciences (BJAS) **print: ISSN 2356–9751**
Vol. (10) Issue (2) (2025), (81-89) **online: ISSN 2356–976x**

https://bjas.journals.ekb.eg/
Applied and Basic Science

Assessment of Trial to Use Exosomes and Salmon DNA with Minoxidil as Multisource Mixture for Hair Follicle Activation an In Vivo Study

Ahmed M. Abdelaziz, Mariam I. El-Gohary, Sara A. El-Akkad, Rahma H. Hagagy, Donia Alaa, Malak A. Ahmed and Ali Saadani
Polygon Research Center, Polygon Technologies Company, Cairo, Egypt.
E-mail: aabdelaziz83@gmail.com

Abstract
Back ground: Hair loss considered the problem affecting on approximately 66% of men aged 35, while approximately 50% of women encounter noticeable hair loss during their lifetime. This study aims to evaluate the use of a mixture of multiple natural sources in addition to a commonly used drug (Minoxidil) and test its effect on modulate hair growth processes *in vivo*. **Methods:** Exosomes were isolated from human cord blood-derived mesenchymal stem cells (MSCs). Exosome characterization was performed using a Zetasizer Nano. Seven groups of C57BL/6 mice were employed as an in vivo model. Experimental groups received the following topical treatments for 10 consecutive days. Histological analysis was conducted using hematoxylin and eosin staining to evaluate hair follicle density, morphology, and distribution. Quantitative analysis of hair follicle number and size was performed using image analysis software. Furthermore, quantitative real-time polymerase chain reaction (qRT-PCR) was employed to assess the relative gene expression levels of Wnt11 and LHX2 genes. **Results:** Histopathology of skin samples demonstrated a significant increase in hair follicle density and elongation in groups treated with minoxidil, with a further moderate enhancement observed in groups receiving combined treatments of exosomes and DNA polynucleotides. Quantitative qRT-PCR analysis of hair follicle tissue revealed a relative down regulation of Wnt 11 and LHX2 genes associated with hair growth inhibition in the minoxidil-treated group. Conversely, the groups treated with exosomes and DNA polynucleotides exhibited a substantial upregulation of genes associated with hair follicle proliferation and differentiation, indicating a potential mechanism for the observed hair growth stimulation. Topical application of the current type exosomes that used in our research is less effective than when combined with minoxidil and salmon DNA. Activity of exosome depending on isolation method and nano size category it is critical point for application. **Conclusion**: Minoxidil alone shows higher hair growth efficacy compared to its combination with exosomes and salmon DNA, results in lower molecular-level expression of hair growth-related genes compared to exosomes.

Key words: minoxidil, exosomes, salmon DNA, cell culture, Wnt 11 and LHX2 genes, hair follicles

1. 1 Introduction

Hair loss, medically termed alopecia, encompasses a diverse range of conditions with multifaceted etiologies. While the exact mechanisms vary, key contributors include genetic predisposition, hormonal imbalances, and environmental factors. Androgenetic alopecia, the most common type, exhibits a strong hereditary component, influenced by androgens like dihydrotestosterone (DHT) [1]. Hormonal fluctuations associated with pregnancy, childbirth, thyroid disorders, and menopause can also significantly impact hair growth cycles. Furthermore, nutritional deficiencies, autoimmune diseases, certain medications, and even excessive stress can disrupt the delicate balance of hair follicle activity, leading to hair thinning or shedding [2]. According to the International Society of Hair Restoration Surgery baldness statistics, the top prescribed hair loss treatments are Finasteride (69%), Minoxidil (53%), and PRP (48%) [3].

Hair growth is a complex process regulated by a multitude of genes. Key players include genes involved in the Wnt/β-catenin signaling pathway, such as Wnt, Lrp5, and β-catenin, which control hair follicle cycling and stem cell activity. Additionally, genes like EDAR and EDARADD, crucial for hair follicle morphogenesis and hair shaft differentiation, play significant roles [4]. The androgen receptor (AR) gene influences hair growth patterns, particularly in males, by mediating the effects of androgens on hair follicles [5]. Moreover, genes encoding keratin proteins, essential components of the hair shaft, contribute to hair strength and structure. Understanding the intricate interplay of these genes provides valuable insights into hair growth disorders and potential therapeutic targets for hair loss treatments [6]. In this study, minoxidil, exosomes and DNA was investigated to determine its capacity to suppress the expression of hair growth-related genes, such as Wnt11 and LHX2.

Minoxidil, a topical medication primarily used to treat androgenetic alopecia, exerts its hair growth-promoting effects through a multifaceted mechanism of action. While the exact mechanisms are not fully understood, it is believed to primarily function by prolonging the anagen phase, stimulating hair follicle cells and increasing blood flow to the scalp [3]. While the precise molecular pathways underlying these effects are still under investigation, it is hypothesized that minoxidil may influence the expression of various genes involved in hair growth, such as those within the Wnt/β-catenin signaling pathway (e.g., Wnt, Lrp5, β-catenin) and genes related to hair follicle cycling and stem cell activity [7].

Exosomes, small extracellular vesicles secreted by cells, have emerged as a promising therapeutic

approach for hair loss. These nanosized vesicles contain various bioactive molecules, including proteins, nucleic acids, lipids, and growth factors, that can modulate cellular communication and tissue regeneration. Here, we will explore the history, mode of action, and reference studies related to exosomes for hair loss [8]. The use of exosomes in regenerative medicine and hair loss treatment is a relatively new area of research. Exosomes were first discovered in the 1980s but gained significant attention in recent years for their regenerative potential. Studies have demonstrated that exosomes derived from various cell types, such as mesenchymal stem cells, adipose-derived stem cells, and dermal papilla cells, can promote hair growth and improve hair follicle function [9]. Exosomes exert their therapeutic effects through multiple mechanisms. They can be taken up by recipient cells, including hair follicle cells, and transfer their cargo of bioactive molecules, such as growth factors, microRNAs, and proteins, to modulate cellular signaling pathways. This can result in increased proliferation, survival, and differentiation of hair follicle cells, leading to improved hair growth. Additionally, exosomes can have anti-inflammatory and immunomodulatory effects, which can help alleviate scalp inflammation and promote a favorable environment for hair follicle growth [10].

Salmon DNA or polydeoxyribonucleotide (PDRN) used in the clinics as anti-aging agent. It consists mainly of DNA fragments derived from the sperm cells of Onco rhynchus mykiss (salmon trout) or Oncorhynchus keta (chum salmon) [11]. The chemical structure of PDRN consists of low molecular weight DNA ranging from 50 to 1 500 kDa. It is composed of a linear polymer of deoxyribonucleotides with phosphodiester linkages in which the monomer units are represented by purine and pyrimidine nucleotides. These polymer chains create a double helix-shaped steric structure. The extraction and purification processes allow for the recovery of more than 95% of pure substance [12].

The introduction of PDRN in clinical practice is not new and its astonishing therapeutic effects include anti-inflammatory, anti-apoptotic, anti-osteoporotic, anti-melanogenetic, anti-allodynic, anti-osteo-necrotic, bone regenerative, tissue damage preventive, anti-ulcerative, wound healing, and scar preventive effects [13]. Owing to its properties with regards to angiogenesis, cell activity promotion, collagen synthesis, anti-inflammation, hyperpigmentation treatment, soft tissue regeneration, and skin priming and revitalization and its anti-aging effect, PDRN has revealed its potential as a promising skin anti-aging agent [14]. The mechanism of action of PDRN involves the activation of the adenosine A2A receptor. Adenosine receptors have been recognized as promising targets for the management of ROS-related disorders which consider one of the main causes of skin aging [15].

2. Methods

Exosomes were isolated from human cord blood-derived mesenchymal stem cells (MSCs) at NAWAH Scientific Company, Egypt according to Nakao et al. (2023) [16]. MSCs were cultured to passage three and harvested at 70% confluency. After washing with phosphate-buffered saline (PBS), cells were cultured in serum-free, low-glucose medium for 48 hours. Subsequently, the culture medium and cells were collected and centrifuged at 2500 rpm for 20 minutes. The supernatant was sequentially filtered through 0.45 µm and 0.22 µm filters. Exosomes were isolated from cell culture supernatant of mesenchymal stem cells derived from umbilical cord blood, biological using an ultrafiltration technique. The size and size distribution of the isolated particles were analyzed using a Malvern nanosizer.

Exosome characterization was performed using a Zetasizer Nano S (Malvern Panalytical, UK) to determine particle size and a BCA Protein Assay Kit (Thermo Fisher Scientific, USA) to quantify exosome concentration.

The extracted genomic DNA was fragmented using according for the DNA extraction protocol of the REME-D kit to an average size of 50 and 1500 bp. Fragment size was confirmed using agarose gel electrophoresis, which showed a uniform distribution of DNA fragments within the desired size range.

Genomic DNA was extracted from 200 mg tissue samples of Salmo salar (Atlantic salmon) utilizing the REME-D commercial kit, employing a modified silica-based spin column method. Tissue samples were homogenized in 1 mL of lysis buffer supplemented with 100 µL of β-mercaptoethanol using vigorous mechanical or manual disruption until complete tissue lysis was achieved. Following homogenization, 400 µL of binding buffer (BB) was added to the lysate, and the mixture was thoroughly mixed. Two sequential 600 µL aliquots of the lysate were transferred to a silica spin column placed within a collection tube and centrifuged at 13,000-14,000 rpm for 1 minute.

The flow-through was discarded after each centrifugation. Subsequently, the remaining lysate was added to the same column and centrifuged for 4 minutes, followed by an additional centrifugation step (1 minute at maximum speed) to ensure complete lysate transfer. The column was then washed sequentially with 500 µL of wash buffers WB1, WB2, and WB3, followed by centrifugation at 13,000-14,000 rpm for 1 minute after each wash to remove impurities. A final centrifugation step at 13,000-14,000 rpm for 5 minutes was performed to remove residual wash buffer. Finally, 50 µL of elution buffer (EB) was added directly to the center of the silica column, and the purified genomic DNA was eluted by centrifugation at 13,000-14,000 rpm for 1 minute after a 4-minute incubation period [17].

Twenty-five 12-week-old male C57BL/6 mice were obtained from NAWAH Scientific Company, Egypt, and housed in a pathogen-free facility in accordance with the Egyptian guidelines for the use of

animal models in research. Following anesthesia, a 1 cm2 area of skin on the dorsal surface of each mouse was shaved. Subsequently, mice were randomly assigned to seven experimental groups (n = 3-4 mice per group): (A) Negative Control (shaved only), (B) Positive Control (shaved with mechanical hair follicle occlusion), (C) Exosomes, (D) Minoxidil, (E) Minoxidil + Exosomes, (F) Minoxidil + Exosomes + Salmon DNA, and (G) Exosomes + Salmon DNA. Minoxidil (5% w/v) was administered topically to C57BL/6 mice. Group D received minoxidil alone, while Groups E and F received minoxidil in combination with exosomes (200 µg/mL) and salmon DNA (118 ng/µL). A volume of 50 µL of the respective treatment was applied daily to the shaved right dorsal skin of each mouse for 10 consecutive days. Following the treatment period, mice were euthanized by [method of euthanasia, e.g., CO2 inhalation]. The dorsal skin of each mouse was harvested and divided into two sections. Section 1 was fixed in 4% paraformaldehyde for subsequent histopathological analysis. Section 2 was preserved in absolute ethanol for further genetic profiling

Skin samples were obtained from C57BL/6 mice in accordance with the international guiding principles for biomedical research involving animals and approved by the veterinary collage at Cairo university in Egypt. Following euthanasia, full-thickness skin biopsies 1 cm2 were collected from the dorsal right flank of each animal. Samples were then divided: one portion was fixed in 10% neutral-buffered formalin for histopathological analysis, The remaining portion of each sample was immediately immersed in RNA later® solution at 4°C for 24 hours to stabilize RNA, followed by storage at -80°C for long-term preservation for subsequent molecular and genetic analyses

Hematoxylin and Eosin (H&E) staining was performed on 4-5 µm thick paraffin-embedded tissue sections. Briefly, slides were deparaffinized in xylene, rehydrated through graded alcohols to distilled water, and stained with Mayer's hematoxylin for 5-10 minutes. After rinsing in tap water, the slides were differentiated in 1% acid alcohol, blued in Scott's tap water, and rinsed again. Subsequently, the slides were counterstained with eosin for 1-2 minutes, dehydrated through graded alcohols, cleared in xylene, and mounted with a coverslip using a permanent mounting medium. [18]. Hair follicles in skin samples (10 images per group at 40X) were counted using HistoMetriX software and images acquired on an Olympus BX series microscope (Japan)

Primers for WNT11 and LHX2 (reference gene) were designed based on published mRNA sequences from NCBI GenBank and optimized for specificity and efficiency using the NCBI BLAST tool. The following primer sequences were used :

WNT11 Forward GCCTGTGAAGGACTCAGAACTTG
WNT11 Reverse AGCTGTCACTGCCGTTGGAAGT
LHX2 Forward GATGCCAAGGACTTGAAGCAGC
LHX2 Reverse GATGCCAAGGACTTGAAGCAGC

RNA extraction :Total RNA was extracted from hair follicle samples using the REME-D Kit following tissue homogenization. RNA quality and quantity were assessed using a Nanodrop spectrophotometer. Within each treatment group, seven samples with the highest average RNA concentration and purity were selected for further analysis. cDNA Synthesis: cDNA was synthesized from 1 µg of total RNA using a reverse transcription kit (iScript™ cDNA Synthesis Kit, Bio-Rad) according to the manufacturer's instructions.

qPCR Analysis: Quantitative real-time PCR (qPCR) was performed using SYBR Green chemistry to quantify the expression of the WNT11 gene. The reaction mixture contained 10 µL of 2x qPCR Master Mix (SYBR Green), 0.4 µL of forward and reverse primers for WNT11 (final concentration 0.2 µM each), 0.4 µL of forward and reverse primers for the reference gene LHX2 (final concentration 0.2 µM each), 6 µL of cDNA, and 3.2 µL of nuclease-free water. qPCR was performed using the following cycling conditions: 95°C for 10 minutes, followed by 40 cycles of 95°C for 15 seconds and 60°C for 1 minute. A melting curve analysis was performed at the end of each run to confirm the specificity of the amplification

3. Results and discussions

Mesenchymal stem cells (MSCs) were successfully isolated from umbilical cord blood and expanded in vitro using standard cell culture techniques. Figure 1 documents the morphological changes observed during the 14-day primary culture and two subsequent 7-day passages, culminating in a confluent MSC monolayer at passage 3. The primary culture, seeded with umbilical cord blood, contained a heterogeneous cell population. However, during this initial 14-day period, a selective adherence process enriched the MSC population. As observed in Figure 1, MSCs readily adhered to the culture flask surface, exhibiting a characteristic transparent appearance when in suspension and adopting a dim, fibroblast-like morphology upon attachment. Non-adherent cells, including hematopoietic cells and other cell types present in the original umbilical cord blood sample, were removed during media changes, effectively enriching the MSC population. This selective adherence is a well-established method for isolating MSCs from various sources, including umbilical cord blood [19].

The subsequent passages (P1 and P2), each lasting 7 days, demonstrated consistent growth kinetics. The attached MSCs reached confluency within this timeframe, maintaining their fibroblast-like morphology (Figure 1). This consistent growth rate across passages suggests the successful establishment of a stable MSC culture. The observed morphology is consistent with previous reports describing umbilical cord blood-derived MSCs [20]. The transparency of the

cells in suspension, transitioning to a dim appearance upon attachment, can be attributed to the cellular changes associated with adherence and spreading, including cytoskeletal reorganization. This morphological transition is a key characteristic used for identifying MSCs in culture [21].

While Figure 1 visually represents the morphological changes and demonstrates the enrichment of MSCs through selective adherence and passaging, further characterization is necessary to confirm their identity and multipotency. Future studies should include analysis of MSC-specific surface markers (e.g., CD73, CD90, CD105) using flow

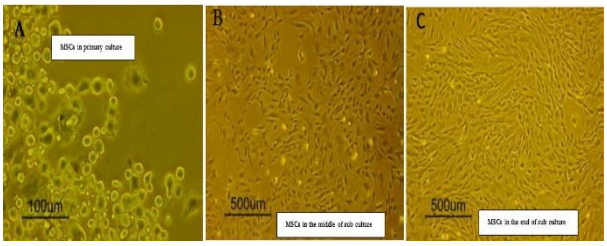

cytometry, as well as assessment of their differentiation potential into various lineages (e.g., adipogenic, osteogenic, chondrogenic) [22]. These experiments will provide crucial data to validate the successful isolation and expansion of MSCs from umbilical cord blood. Furthermore, the growth kinetics observed in this study (7 days to confluency per passage) provide a baseline for future experiments involving these cells.

Figure (1) Illustrates the morphology of MSC at various stages. (A) During primary culture, the cells are mostly in suspension with a limited number attached. (B) The attached cell population expands, with most cells adhering to the culture surface, though not yet confluent. (C) The cells achieve approximately 85% confluency, forming a complete, attached layer. All images were captured using an inverted microscope at both 4X and 20X magnification.

The differentiation of MSCs towards the osteogenic lineage was assessed by culturing cells in conditioned media supplemented with dexamethasone, β-glycerophosphate, and ascorbic acid for a defined period (the duration should be specified in your methods). Following this incubation period, Alizarin Red S staining was performed to visualize calcium deposition, a hallmark of osteogenic differentiation. As shown in figure 2, cells cultured in the osteogenic differentiation media exhibited distinct red patches, indicative of calcium mineral formation. This staining is a result of Alizarin Red S binding to calcium ions, forming a red calcium-alizarin complex [23]. The intensity of the red staining is often correlated with the degree of mineralization and, consequently, the extent of osteogenic differentiation. In contrast, the control group, cultured in standard growth media without the osteogenic supplements, showed no Alizarin Red S staining, confirming the specificity of the staining for mineralized calcium deposits.

In addition to the biochemical evidence of osteogenic differentiation provided by Alizarin Red S staining, morphological changes were also observed (Figure 2). MSCs cultured in the osteogenic differentiation media displayed a characteristic spindle-shaped morphology. This morphological transition from the typical fibroblast-like shape of undifferentiated MSCs to a more elongated, spindle-like shape is a common observation during osteogenic differentiation [24]. The spindle shape is associated with the reorganization of the cytoskeleton and the expression of osteoblast-specific genes [25]. Conversely, cells in the control group retained their original, more spread-out, fibroblast-like morphology, consistent with their undifferentiated state.

The combined evidence of Alizarin Red S staining and the observed morphological changes strongly suggests that the conditioned media containing dexamethasone, β-glycerophosphate, and ascorbic acid effectively induced osteogenic differentiation of the MSCs. The presence of red patches in the Alizarin Red S staining indicates calcium deposition, a key functional characteristic of osteoblasts. The accompanying spindle-shaped morphology further supports this interpretation.

While these results provide compelling evidence of osteogenic differentiation, it is important to note that Alizarin Red S staining provides a qualitative or semi-quantitative assessment of calcium deposition. For a more quantitative analysis, techniques such as measuring calcium content using a colorimetric assay or quantifying the expression of osteogenic markers (e.g., RUNX2, OCN, ALP) using RT-qPCR or other

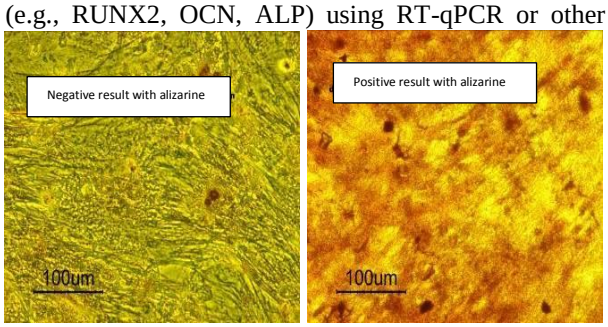

molecular biology methods would be beneficial [26].

Figure (2) Depicts MSCs stained with alizarin red S. Panel (A) shows the control group, which yielded negative results, while panel (B) shows the test group with positive results, evidenced by prominent red patches.

The isolated exosomes were analyzed using a Malvern nanosizer (Figure 3). This analysis revealed a heterogeneous population of particles, with sizes ranging from 70 nm to 600 nm. While a substantial proportion (approximately 50%) of the particles measured below 300 nm, a size range commonly

associated with exosomes. Following ultrafiltration, the isolated particles were concentrated to 200 µg/ml, as determined by a BCA protein assay. This protein concentration provides a standardized measure of the exosome preparation.

The size heterogeneity observed in our preparation is not unexpected. Although ultrafiltration was employed, it is known that this technique, while effective in enriching exosomes, may not provide absolute purity. Other micro vesicles, such as shedding micro vesicles or apoptotic bodies, can have overlapping size ranges with exosomes and may be present in the final preparation [27]. The presence of larger particles (>300 nm) could also indicate some degree of aggregation of the exosomes or other micro vesicles during the isolation or concentration process. Aggregation can be influenced by factors such as buffer composition, pH, and storage conditions.

While the presence of larger particles suggests potential impurity, the significant proportion of particles below 300 nm, coupled with the protein concentration measurement, provides reasonable evidence for the enrichment of exosomes in our preparation. However, for more rigorous characterization and to increase confidence in the exosome population, future studies could incorporate additional purification steps, such as size-exclusion chromatography (SEC) or density gradient ultracentrifugation, which are known to provide higher purity exosome preparations [28].

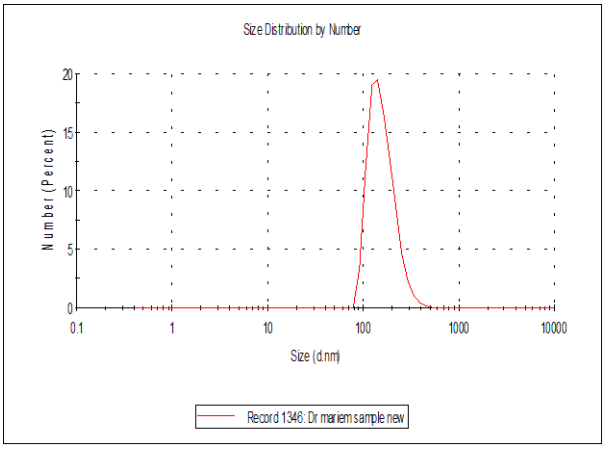

Figure (3) The size distribution of the isolated particles, as measured by a Malvern nanosizer

Hematoxylin and eosin (H&E) staining was employed to visualize and quantify hair follicle density and distribution in skin samples across all experimental group; Summarized in figure 5. Microscopic examination of the negative control group (A) revealed normal hair follicle histology, characterized by a typical range of follicle numbers and distribution. This baseline observation provides a context for evaluating the effects of the various treatments. In stark contrast, the positive control group (B) exhibited a substantial reduction in the number of hair follicles, demonstrating the efficacy of the positive control intervention in inducing hair loss or follicle regression. This reduction serves as a positive control, confirming the experimental setup's ability to detect changes in hair follicle density.

Among the treatment groups, Group C, receiving exosomes only, displayed the lowest hair follicle count, with only a few follicles observed. This suggests that exosomes alone, under the conditions of this study, had a limited effect on promoting hair follicle growth or preventing hair loss. Conversely, Group D, treated with minoxidil, demonstrated the most pronounced stimulatory effect on hair follicle growth, exhibiting the highest follicle count and numerous newly formed hair follicles. This finding is consistent with the known hair growth-promoting properties of minoxidil and validates its inclusion as a positive control for hair follicle stimulation [29].

Groups E, F, and G, which received combined treatments, presented an interesting pattern. Group E received minoxidil and exosomes, Group F received minoxidil, exosomes, and salmon DNA, and Group G received exosomes and salmon DNA. All three groups showed a moderate number of hair follicles. Importantly, the follicle counts in these combined treatment groups did not exceed those observed in the minoxidil-only group (D). This suggests that the addition of exosomes and/or salmon DNA to minoxidil did not further enhance the stimulatory effect on hair follicle growth. While the combined treatments did not appear to have an additive effect compared to minoxidil alone, they did maintain a moderate level of hair follicle density, suggesting that they may have some positive influence. However, this influence was not statistically different from minoxidil alone.

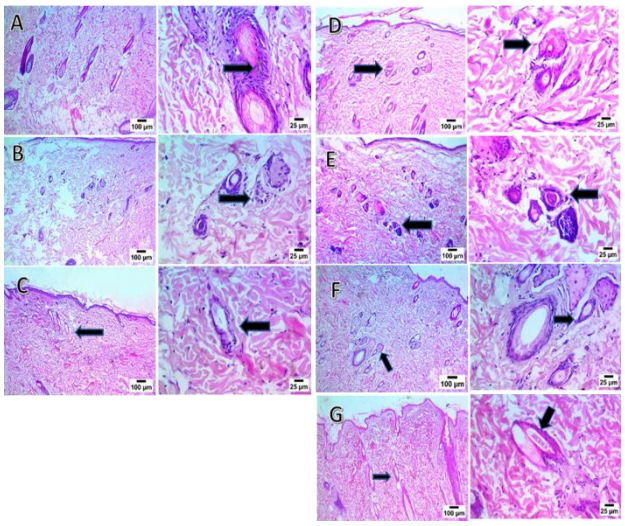

Figure (4) Presents-stained skin samples using Hematoxylin and Eosin. Each group is summarized in two images captured at 100x and 400x magnification. Histological analysis revealed normal hair follicle structure with varying numbers in the negative control group (A). A marked decrease in hair follicle number

was observed in the positive control group (B). Group C (exosomes) presented a low number of hair follicles. Group D (minoxidil) demonstrated a high number of newly formed hair follicles. Groups E (minoxidil + exosomes), F (minoxidil + exosomes + salmon DNA), and G (exosomes + salmon DNA) exhibited a moderate number of hair follicles.

Figure (5) Displays photographic images for all groups, including images at day zero. Each group is represented by two images taken on days 5 and 10. In Group A (negative control group), hair was removed by shaving. Group B (positive control group) had hair follicles plucked along with the hair. Group C (exosomes) shows less hair growth compared to the standard groups, while Group D (minoxidil) exhibits a significant increase in newly formed hairs. Groups E (minoxidil + exosomes), F (minoxidil + exosomes + salmon DNA), and G (exosomes + salmon DNA) demonstrated moderate hair growth stages when compared to the minoxidil group

The qPCR data represented in figure 6 and table 1

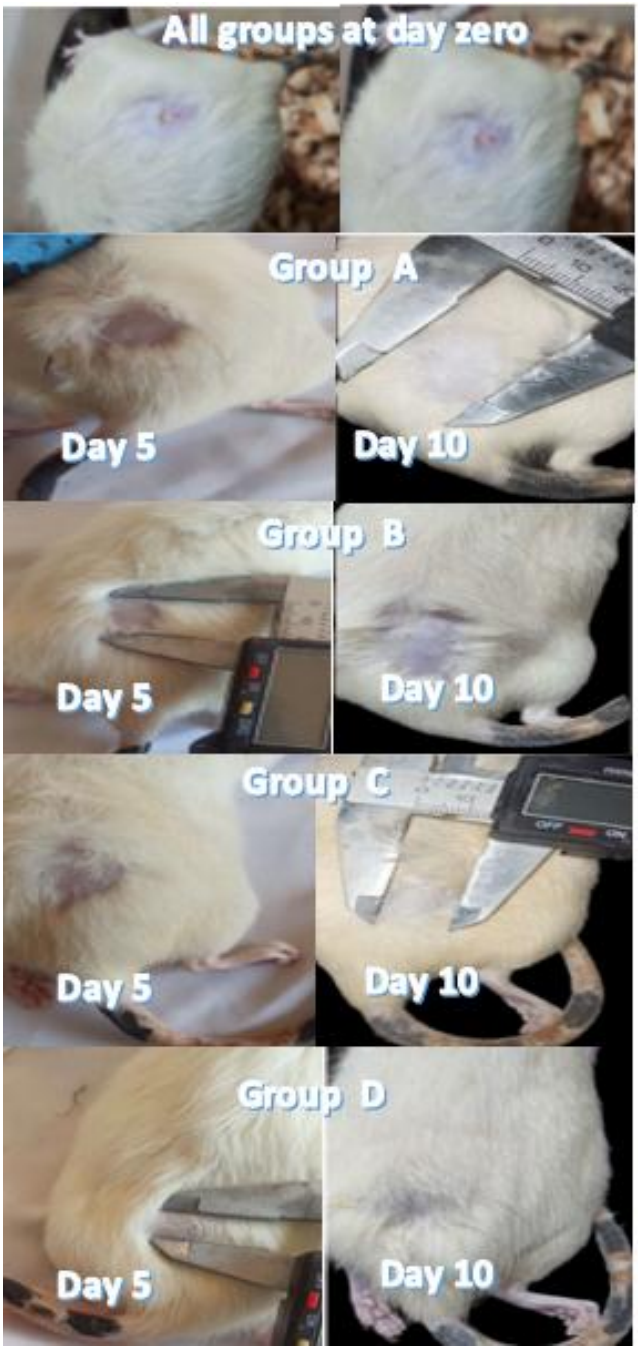

provide information on the gene expression of WNT11 and LHX2. The observation that WNT11 has higher gene expression in the samples than LHX2 is interesting. Gene expression levels were quantified using real-time PCR. To correct for differences in starting RNA amounts, cDNA synthesis efficiency, and variations between PCR runs, Ct values for the target gene (WNT11) were normalized to the Ct values of the stably expressed housekeeping gene LHX2. LHX2 was chosen as a reference gene because in this study for normalization of qPCR data. While commonly employed reference genes like ACTB and GAPDH are frequently utilized in gene expression studies, their suitability can vary depending on the specific tissue, experimental conditions, and target genes under investigation [30]. LHX2, a transcription factor involved in developmental processes [31], was chosen due to its potential for stable expression in skin tissue and its limited prior use as a reference gene in hair follicle research. This latter point was considered an advantage, as it potentially reduces the risk of co-regulation with the WNT family genes, which are central to our investigation [32]. However, it is crucial to acknowledge that LHX2 is not a universally validated reference gene, particularly in the context of hair follicle studies. Therefore, rigorous validation of LHX2 stability across all experimental conditions was performed, as detailed in the subsequent section, to ensure the reliability of our gene expression data [33].

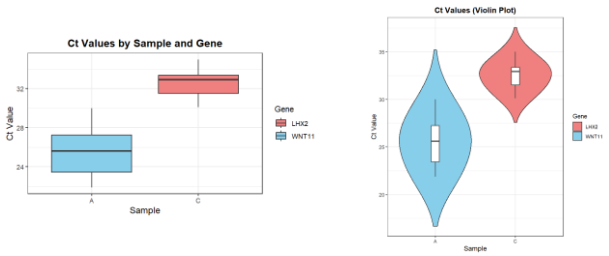

Figure (6) Gene expression of WNT11 and LHX2 by using boxplot and violin plot shows that the WNT11 has high gene expression in the samples than LHX2 gene in the samples

Table (1) Relative change in gene expression compared to a control and expression fold change using the 2 genes (the housekeeping and targeting gene) from real time PCR data

Average Experimental Ct Value	Average Experimental Ct Value2	Average Control Ct Value	Average Control Ct Value2	ΔCt Value ((Experimental	Ct Δ Value ((Control	CT ΔΔ value	expression fold change
TE	HE	TC	HC	ΔΔCTE	ΔΔCTC	ΔΔCT	2^-(ΔΔCT)
26.81	32.93	22.1	30.12	-6.12	-8.02	1.9	-1.052631579
24.76	31.63	22.1	30.12	-6.87	-8.02	1.15	-1.739130435
30	33.35	22.1	30.12	-3.35	-8.02	4.67	-0.428265525
27.68	35	22.1	30.12	-7.32	-8.02	0.7	-2.857142857
21.88	33.4	22.1	30.12	-11.52	-8.02	-3.5	0.571428571
25.6	31.38	22.1	30.12	-5.78	-8.02	2.24	-0.892857143

To quantify the relative changes in WNT11 gene expression, the 2^-(ΔΔCT) method was employed. This method is a widely used approach for relative quantification in real-time PCR, as it accounts for variations in starting RNA amounts, cDNA synthesis efficiency, and PCR run variability [30]. First, the Ct values of the target gene (WNT11) were normalized to the endogenous control gene (LHX2) within each sample by calculating the difference between their respective calculations the differences between experimental values (TE – HE) and the control values (TC – HC). The ΔCt values for the experimental (ΔCTE) and control (ΔCTC) conditions, respectively [34].

This normalization step corrects for potential differences in sample preparation and technical variation. Next, to determine the relative change in gene expression compared to the control group, the difference between each sample's ΔCt value and the average ΔCt value of the control group was calculated Then, calculate the difference between the ΔΔCT values for the experimental and the control conditions (ΔΔCTE – ΔΔCTC). Finally, the fold change in gene expression was calculated using the formula (2^-(ΔΔCT)). This calculation yields a value representing the fold difference in WNT11 expression between each sample and the control, where a value of 1 indicates no difference, values greater than 1 indicate increased expression, and values less than 1 indicate decreased expression [34].

In gene expression studies using qPCR, observed differences in Ct values or calculated fold changes can arise due to various factors, including biological variation, technical variability, and experimental noise. Therefore, statistical analysis is crucial to distinguish true biological effects from random fluctuations. To address this, normalized Ct values were analyzed using t-test for comparison between two groups, One-way ANOVA followed by an appropriate post-hoc test, A p-value of less than 0.05 was adopted as the threshold for statistical significance, indicating a 95% confidence level that the observed difference is not due to chance [35].

5. Conclusion

Using multiple natural sources, either alone or in combination with known medications, is an effective method for solving many hair loss problems. The current study has shown results that have alarm to researchers in this field to carefully select the source of exosomes and conduct a comprehensive study to characterize it before use. The injection method is also an important factor in determining its effectiveness.

6. References

[1] Thibaut, S., & Tobin, D. J. (2023). Androgenetic alopecia: A comprehensive

review. Journal of the American Academy of Dermatology, 89(1), 13-30

[2] Hamza, O. A., & Hordinsky, M. K. (2019). Hair loss disorders: Pathogenesis, diagnosis, and management. Journal of the American Academy of Dermatology, 80(1), 1-19.

[3] Gupta AK, Talukder M, Venkataraman M, Bamimore MA. Minoxidil: a comprehensive review. J Dermatolog Treat. 2022 Jun;33(4):1896-1906.

[4] Cotsarelis, G., Sun, T., & Lavker, R. M. (2001). Hair Follicular Stem Cells: From Signaling Pathways to Skin Regeneration. Cell, 107(1), 13–24.

[5] Hebert, J. M., Higgins, M. J., & Kaufman, K. D. (2000). Androgenetic Alopecia: Pathophysiology and Management. American Family Physician, 61(1), 165–174.

[6] Nyström, L., & Stenn, K. S. (2010). Hair Follicle Stem Cell Biology and Diseases. Cell Stem Cell, 6(4), 387–397.

[7] Messenger AG, Rundegren J. Minoxidil: mechanisms of action on hair growth. Br J Dermatol. 2004;150(2):186–94.

[8] Zhang, J, Liu X, Li H, et al. Exosomes/tricalcium phosphate combination scaffolds can enhance bone regeneration by activating the PI3K/Akt signaling pathway. Stem Cells Transl Med. 2017;6(10):1806-1818.

[9] Zhang, L, Zhang S, Yao J, Pang J, Ma X, Guo C, et al. (2019). Exosomes: A novel platform for drug delivery in regenerative medicine. J Control Release. 299: 109–121.

[10] Li, W, Mu D, Tian F, et al. Exosomes derived from mesenchymal stem cells inhibit apoptosis and promote hair follicle stem cell proliferation and differentiation. Int J Mol Sci. 2019;20(15): 3751

[11] Squadrito, F, Bitto A, Irreraa N, et al. Pharmacological activity and clinical use of PDRN. Front Pharmacol. 2017; 8:224.

[12] Belmontesi, M. Polydeoxyribonucleotide for the improvement of a hypertrophic retracting scar-An interesting case report. J Cosmet Dermatol. 2020;19(11): 2982–2986.

[13] Yoon, S, Kang JJ, Kim J, et al. Efficacy and safety of intra-articular injections of hyaluronic acid combined with polydeoxyribonucleotide in the treatment of knee osteoarthritis. Ann Rehabil Med. 2019;43(2):204–214.

[14] Lee, DW, Hyun H, Lee S, et al. The effect of polydeoxyribonucleotide extracted from salmon sperm on the restoration of bisphosphonate-related osteonecrosis of the jaw. Mar Drugs. 2019;17(1):51.

[15] Irrera, N, Arcoraci V, Mannino F, et al. Activation of A2A receptor by PDRN reduces neuronal damage and stimulates WNT/β-CATENIN driven neurogenesis in spinal cord injury. Front Pharmacol. 2018; 9:506.

[16] Nakao, M., Matsui, M., Kim, K. et al. Umbilical cord-derived mesenchymal stem cell sheets transplanted subcutaneously enhance cell retention and survival more than dissociated stem cell injections. Stem Cell Res Ther 14, 352 (2023)

[17] Johnston, A. E., Armstrong, M. A., & Muir, J. F. (2002). A rapid and efficient method for DNA extraction from salmon eggs for microsatellite analysis. Aquaculture Research, 33, 113-116.

[18] Bancroft, J. D., & Gamble, M. (2008). Theory and Practice of Histological Techniques. Churchill Livingstone.

[19] Dominici, M., Le Blanc, K., Mueller, I., et al. (2006). Minimal criteria for defining multipotent mesenchymal stromal cells from tissues. Cytotherapy, 8(4), 315-317

[20] Troyer, D. L., & Weiss, M. L. (2010). Concise Review: Umbilical Cord Blood Mesenchymal Stem Cells: Biology, Potential, and Clinical Application. Stem Cells Translational Medicine, 1(1), 71-80.

[21] Vicente-Yáñez, S. F., Buckley, C., López-Cabrera, F., et al. (2015). Cell adhesion and spreading. Advances in Protein Chemistry and Structural Biology, 98, 1-49.

[22] International Society for Cellular Therapy. (2018). Mesenchymal Stromal Cells: A Consensus Statement on Nomenclature and Criteria for Minimal Definitions. Cytotherapy, 20(9), 1083-1085.

[23] Gregory, C. A., Gunn, J., Hickey, P., et al. (2004). The use of alizarin red to quantify mineralization in cultured cells. Analytical Biochemistry, 325(2), 267-273.

[24] Luo, F., Liu, L., Tang, Y., et al. (2021). A Review of Osteogenesis Signaling Pathways in Mesenchymal Stem Cells. Frontiers in Cell and Developmental Biology, 9, 655459.Owen, T. A.,

[25] Franceschi, R. T., Dwivedi, P., D'Souza, R. N., et al. (2003). Transcriptional control of osteoblast differentiation. Journal of Cellular Biochemistry, 88(2), 253-264.

[26] Bieler, R. A., Wagner, A., Saffrich, R., et al. (2010). Quantitative assessment of osteogenesis in cultures of mesenchymal stem cells using real-time reverse transcription-polymerase chain reaction. Tissue Engineering Part C: Methods, 16(6), 1481-1489.

[27] Shao, B., Yamamoto, T., Toyooka, T., et al. (2018). A comprehensive review of extracellular vesicle isolation methods. Journal of Extracellular Vesicles, 7(1), 1464206.

[28] Lötvall, J., Hill, A. F., Burdach, S., et al. (2015). Minimal experimental requirements for definition of extracellular vesicles and their

targets: a position statement from the International Society for Extracellular Vesicles. Journal of Extracellular Vesicles, 4, 26928.

[29] Yu CQ, Zhang H, Guo ME, Li XK, Chen HD, Li YH, Xu XG. Combination therapy with topical minoxidil and nano-microneedle-assisted fibroblast growth factor for male androgenetic alopecia: a randomized controlled trial in Chinese patients. Chin Med J (Engl). 2020 Nov 5;134(7):851-853.

[30] Bustin. SA, "Standardization of qPCR and RT- qPCR." Genet Eng Biotechnol News 29.14 (2009).

[31] Watson, B. A., Feenstra, J. M., Van Arsdale, J. M., Rai-Bhatti, K. S., Kim, D. J., Coggins, A. S., ... & Oberg, K. C. (2018). LHX2 mediates the FGF-to-SHH regulatory loop during limb development. Journal of developmental biology, 6(2), 13.

[32] Wu, J., Li, W., Lin, C., Chen, Y., Cheng, C., Sun, S., & Li, H. (2016). Co-regulation of the Notch and Wnt signaling pathways promotes supporting cell proliferation and hair cell regeneration in mouse utricles. Scientific reports, 6(1), 29418.

[33] Folgueras, A. R., Guo, X., Pasolli, H. A., Stokes, N., Polak, L., Zheng, D., & Fuchs, E. (2013). Architectural niche organization by LHX2 is linked to hair follicle stem cell function. Cell stem cell, 13(3), 314-327.

[34] Livak, K. J., & Schmittgen, T. D. (2001). Analysis of relative gene expression data using real-time quantitative PCR and the $2^{-\Delta\Delta CT}$ method. methods, 25(4), 402-408.

[35] Sirak, B. (2025). The Impact of Atorvastatin on Gene Expression in SiMa cells.